

Role of defects on the electronic and magnetic properties of CrAs/InAs and CrAs/CdSe half-metallic interfaces

I. Galanakis* and I. Lekkas

Department of Materials Science, School of Natural Sciences, University of Patras, GR-26504 Patra, Greece

Abstract

We present an extended study of single impurity atoms at the interface between the half-metallic ferromagnetic zinc-blende CrAs compound and the zinc-blende binary InAs and CdSe semiconductors in the form of very thin multilayers. Contrary to the case of impurities in the perfect bulk CrAs studied in [I. Galanakis and S.G. Pouliasis, *J. Magn. Magn. Mat.* 321 (2009) 1084] defects at the interfaces do not alter in general the half-metallic character of the perfect systems. The only exception are Void impurities at Cr or In(Cd) sites which lead, due to the lower-dimensionality of the interfaces with respect to the bulk CrAs, to a shift of the p bands of the nearest neighboring As(Se) atom to higher energies and thus to the loss of the half-metallicity. But Void impurities are Schottky-type and should exhibit high formation energies and thus we expect the interfaces in the case of thin multilayers to exhibit a robust half-metallic character.

Key words: Electronic structure, Half-metals, CrAs

PACS: 75.47.Np, 75.50.Cc, 75.30.Et

1. Introduction

The discovery of Giant Magnetoresistance in 1998 by the groups of Fert and Grünberg led to new reading heads for hard disks [1,2]. Moreover for the first time, a device based on magnetic phenomena replaced a conventional electronics device based on the movement of the electrons charge and thus opened the way to the field of spintronics or magnetoelectronics. The aim is to replace conventional electronics with new devices where magnetism plays a central role leading to smaller energy consumption. Several architectures have been proposed [3,4] but only in 2009 Dash and collaborators managed to inject spin-polarized current from a metallic electrode into Si, which is a key issue in current research

in this field. showing that spintronic devices can be incorporated into conventional electronics [5].

In order to maximize the efficiency of spintronic devices, the injected current should have as high spin-polarization as possible [3,4]. To this respect half-metallic compounds have attracted a lot of interest (for a review see reference [6]). These alloys are ferromagnets where the majority spin channel is metallic while the minority-spin band structure is that of a semiconductor leading to 100% spin-polarization of the electrons at the Fermi level and thus to possibly 100% spin-polarized current into a semiconductor when half metals are employed as the metallic electrode. The term half-metal was initially used by de Groot et al in the case of the NiMnSb Heusler alloy [7].

Ab-initio (also known as first-principles) calculations have been widely used to explain the properties of these alloys and to predict new half-metallic

* Corresponding author. Phone +30-2610-969925, Fax +30-2610-969368

Email address: galanakis@upatras.gr (I. Galanakis).

compounds. An interesting case is the transition-metal pnictides like CrAs and MnAs. Akinaga and collaborators found in 2000 that when a CrAs thin film is grown on top of a zinc-blende semiconductor like GaAs, the metallic film adopts the lattice of the substrate and it crystallizes in a meta-stable half-metallic zinc-blende phase [8] structure. Later CrAs was successfully synthesized in the zinc-blende structure in the form of multilayers with GaAs [9] and other successful experiments include the growth of zinc-blende MnAs in the form of dots [10] and CrSb in the form of films [11,12].

Experiments agree with predictions of ab-initio calculations performed by several groups [13,14,15,16]. In the case of the half-metallic ferromagnets like CrAs or CrSe, the gap in the minority-spin band arises from the hybridization between the p -states of the sp atom and the triple-degenerated t_{2g} states of the transition-metal and as a result the total spin-moment, M_t , follows the Slater-Pauling (SP) behavior being equal in μ_B to $Z_t - 8$ where Z_t the total number of valence electrons in the unit cell [13]. Recently theoretical works have appeared attacking also some crucial aspects of these alloys like the exchange bias in ferro-/antiferromagnetic interfaces [17], the stability of the zinc-blende structure [18], the dynamical correlations [19], the interfaces with semiconductors [20,21], the exchange interaction [22], the emergence of half-metallic ferromagnetism [23] and the temperature effects [24]. An extended overview on the properties of these alloys can be found in reference [25].

Recently we have published a work on the role of defects in the case of half-metallic CrAs, CrSb and CrSe alloys crystallizing in the zinc-blende structure and adopting the lattice constant of InAs binary semiconductor of 0.606 nm [26]. All defects under study in this reference, with the exception of void impurities at Cr and sp sites and Cr impurities at sp sites, were found to induce new states within the gap and the Fermi level can be pinned within these new minority states destroying the half-metallic character of the perfect bulk compounds. These impurity states are localized in space around the impurity atoms and very fast the bulk behavior is regained. But in realistic devices interfaces with semiconductors will occur and the interaction of these bulk-impurity states with interface states can destroy the spin-polarization of the injected current. Ab-initio calculations show that interfaces are in principle half-metallic for pnictides containing Cr or V atoms even when the semiconductor is a II-VI

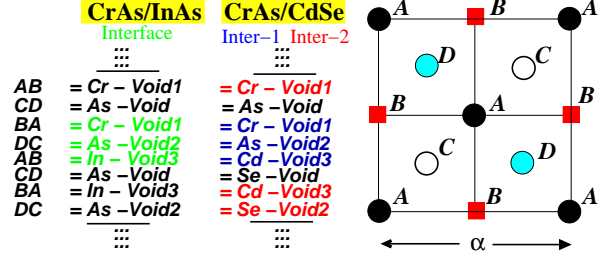


Fig. 1. (Color online) Schematic representation of the structure of the multilayers under study. We have assumed that the growth direction of the zinc-blende structure is the (001) and the period consists of four CrAs and four InAs(CdSe) layers. Each plane contains atoms of a single chemical type plus a void site. We denote as Void1 the vacant site in the same layer with the Cr atoms at the interfaces, Void2 in the interfacial As(Se) layer and Void3 in the interfacial In(Cd) layer. The distance between two consecutive plane is $\frac{1}{4}$ of the lattice constant. Note that in the case of the CrAs/CdSe we have two non-equivalent interfaces: (i) when the sequence of the atoms is ...-Cr-As-Cd-... denoted as CrAs/CdSe-1 and (ii) when the sequence is ...-Cr-Se-Cd-... denoted as CrAs/CdSe-2. Finally we should note that we have assumed the lattice constant of the two semiconductors (0.606 nm).

like CdSe and not a III-V one like InAs, and no interface states occur [20]. But impurities at the interfaces can induce new impurity-interfaces states within the minority spin-gap which can couple to the bulk impurity states and lead to loss of the half-metallic character.

In this communication we expand our previous study to cover also the case of impurities at interfaces. We have decided to consider CrAs as the half-metallic spacer since it is the most-widely studied transition-metal zinc-blende pnictide and both InAs and CdSe as the zinc-blende semiconducting spacer to cover both the case of III-V and II-VI semiconductors. In and Cd atoms, as well as As and Se atoms, are in the same row of the periodic table and they have one valence electron difference and thus both alloys have the same lattice constant of 0.606 nm and for this value of the lattice constant bulk CrAs shows a Fermi level exactly in the middle of the minority-spin gap making clear the appearance of impurity states. For our calculation we employ the the Korringa-Kohn-Rostoker method (KKR) method [27] as in the case of the perfect bulk [13] and interfaces [20] and we have treated the impurities as in references [26,28].

To model the interface we have considered a multilayer with a period of 4 CrAs and 4 InAs(CdSe) monolayers (MLs) which is in accordance with the experimental data in reference [9] and a schematic

Table 1

Atom-resolved spin magnetic moments in μ_B for the perfect CrAs and CrSe alloys and for the three perfect multilayers under study. For the position of each atom in the multilayer please refer to figure 1.

Perfect Systems	CrAs(Bulk)	CrSe(Bulk)	CrAs/InAs	CrAs/CdSe-1	CrAs/CdSe-2
Cr	3.267	3.825	3.248	3.117	3.462
Void1	-0.029	0.049	-0.008	-0.025	-0.002
As(Se) [CrAs layer]	-0.382	-0.103(Se)	-0.383	-0.388	
As(Se) [Interface]			-0.209	-0.365	-0.093(Se)
As(Se) [SemiConducting layer]			-0.066		-0.048(Se)
Void2	0.080	0.162	0.043	0.027	0.056
In(Cd)			-0.008	-0.045	0.003
Void3			-0.022	-0.033	-0.001

illustration is shown in figure 1. As growth direction we have chosen the (001) and thus its layer is made up of atoms of a single chemical type. Moreover at each layer we have considered a void to describe better the space in our calculation. In the case of CrAs/InAs multilayers all interfaces are equivalent while in CrAs/CdSe case we have two non-equivalent interfaces; the interface where As is between the Cr and Cd layers which we denote as Interface-1 and the interface where Se separates the Cr and Cd layers (Interface-2). Moreover we should note that the distance between two successive layers is $1/4$ of the lattice constant and thus atoms in successive layers are nearest atoms while within the same atomic layer the nearest atoms are second neighbors. We have also denoted as Void1 the vacant site at the Cr interface layer, Void2 in the As(Se) interface layer and Void3 in the In(Cd) interface layer. We have considered all possible impurities and in section 2 we present the case of perfect bulk and multilayers while in section 3 we present the properties of the Cr impurities at various sites at the interface, in section 4 the case of As(Se) impurities, in section 5 the case of voids and in section 6 the case of In(Cd) impurities. Finally in section 7 we summarize and conclude. Throughout the discussion we compare our results with the case of impurities in perfect bulk CrAs presented in reference [26]. In the case of the CrAs/CdSe-2 interface the Cr atoms have As atoms from one side and Se atoms from the other side but as it was shown in [26] both CrAs and CrSe show similar behavior with respect to the defects-induced states.

2. Perfect systems

We will start our discussion from the perfect systems. In table 1 we have gathered the atom-resolved spin magnetic moment in μ_B for the three interfaces and for the bulk CrAs and CrSe alloys. Notice that for the bulk systems, where we have two vacant sites, we denote as Void1 the vacant site with the same symmetry as the Void1 site at the interface and the same stands for the Void2 site. Bulk CrAs has 11 valence electrons per unit cell while CrSe has 12 valence electrons and thus half-metallic CrAs has a total spin moment of $3 \mu_B$ and CrSe of $4 \mu_B$. As it was shown in [13] Cr atoms in CrSe accommodate half of the extra electron in the majority-spin band leading to a larger Cr-spin moment which now reaches about $3.8 \mu_B$ instead of $\sim 3.3 \mu_B$ in CrAs. The other half electron is accommodated in the majority-spin band of the Se and Void2 atoms as it easily deduced from the spin moments presented in table 1 (Void2 is not a real atom but orbitals from the nearest Cr atoms penetrate in the Void2 site).

In the case of the CrAs/InAs multilayer, both Cr atoms have exactly the same nearest environment as in bulk CrAs and almost an identical spin magnetic moment. The same is true also for the As atom within the CrAs layer (As layer between the two Cr layer as shown in figure 1) which has four Cr and four Void1 sites as nearest neighbors as in the bulk CrAs and exactly the same spin magnetic moment of $-0.38 \mu_B$. As at the interface layer has one Cr layer from one side an In layer from the other side. In atoms have two valence electrons which mainly are of s character and have no contribution to the In spin magnetic moment. The spin moment at the In sites is induced by the As atoms since p -orbitals of As

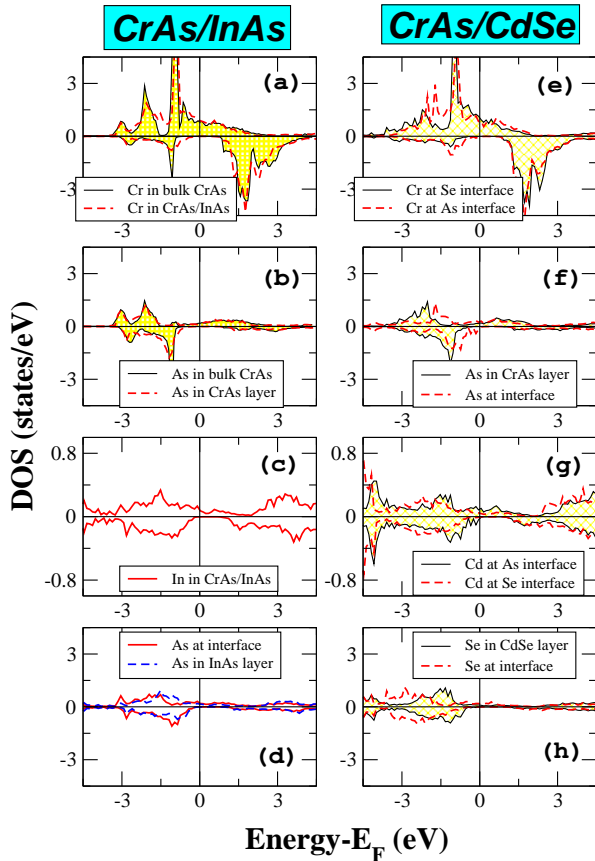


Fig. 2. (Color online) Atom-resolved density of states (DOS) for the bulk CrAs and the perfect multilayers under study presented in figure 1. Panels (a), (b), (c) and (d) refer to the CrAs/InAs multilayer and (e), (f), (g) and (h) to the CrAs/CdSe multilayer. In panel (a) and (b) we have also included the DOS of Cr and As atoms in perfect bulk CrAs for comparison. Note that in the case of the CrAs/CdSe we have two interfaces one containing As one containing Se atoms (see figure 1 for explanation). The Fermi energy has been set as the zero of the energy axis. Positive DOS values correspond to the spin-up (majority-spin) electrons and negative values to the spin-down (minority-spin) electrons.

penetrate in the In sites. Thus As atoms at the interface show a smaller absolute value of the spin magnetic moment since now they have only two instead of four Cr nearest neighbors (the spin-moment at As is induced by the Cr atoms through the hybridization of the As- p and Cr- t_{2g} states) and In atoms at the interface show a negligible spin moment induced by the As interface atoms which in reality is the reflection of the Cr spin moment. As atoms within the semiconducting layer have four In atoms as nearest neighbors and a very small spin magnetic moment.

In the case of the CrAs/CdSe multilayer we have two inequivalent interfaces and the two Cr layer are

no-more equivalent. The Cr atoms at the As interface behave similarly to bulk CrAs although the spin moment is somewhat smaller while in the case of the Se interface Cr atoms have two As and two Se atoms as nearest neighbors exhibiting a spin magnetic moment of about $3.5\mu_B$ a mean value between the bulk CrAs and CrSe atoms. Within the CrAs layer As shows a spin magnetic moment similar to the CrAs/InAs multilayer. At the 1st interface As atoms show similar behavior to the CrAs/InAs case although their spin moment is larger in absolute value since Cd atoms have one valence electron less than In ones and the leakage of charge from the As interface atoms to the Cd ones is smaller than to the In ones. In the 2nd interface Se atoms have one electron more than As one and thus the Se- p orbitals are less polarized from the Cr- t_{2g} ones and show a smaller spin magnetic moment by a factor of four. Within the CdSe semiconducting layer the Se atoms behave like the As atoms in the InAs layer in the first interface and show a small value of the spin moment. Finally Cd atoms show a negligible spin-magnetic moment as the In ones.

In figure 2 we have gathered the density of states (DOS) in states/eV for both multilayers under study and the bulk CrAs. In the left column we present the case of the CrAs/InAs multilayer. Cr atoms at the interface show a similar DOS to the bulk case with a very small weight of occupied minority-spin states while in the majority band both e_g and a fraction of the three t_{2g} states are occupied. The gap is smaller in the case of the multilayer since the occupied minority-spin states are broader in energy and this is reflected to all other atoms. As atoms within the CrAs layer show an almost identical DOS to the bulk CrAs case as was also the case for the spin magnetic moments. As we move to the interface and then to the InAs layer the shape of the As states changes due to the different local environment and the bands move towards the Fermi level. The states shown are the p states since the s -states of all atoms are located at about -9 to -12 eV below the Fermi level and are not shown in the figures. Note that for the In atoms we have used a different scale in the vertical axis. In the case of the CrAs/CdSe multilayer the half-metallicity is again present as for the CrAs/InAs layer but due to the character of the II-VI semiconductor the gap in the minority-spin band is smaller and the Fermi level is near the left-edge of the gap as it is clearly seen in the case of the Cr DOS. The reduction of the gap-width is larger for the As than the Se interface and this agrees with

Table 2

Atom-resolved spin magnetic moments for the case of Cr impurity atoms at interfacial As(Se) and Void2 sites in the case of bulk CrAs and the three interfaces under study. "imp" stands for impurity and "1st" stands for nearest neighbor atoms (similar for 2nd and 3rd). We present results for both cases of coupling of the Cr impurity spin moment with respect to the spin moments of the Cr nearest-neighbors (ferromagnetic-FM and antiferromagnetic-AFM cases). Note that As(Se) atoms can be found in the CrAs layer [CrAs], the interfaces [Inter] and the semiconducting layer [SC].

Cr at As(Se) site	BULK CrAs		CrAs/InAs		CrAs/CdSe-1		CrAs/CdSe-2	
	FM	AFM	FM	AFM	FM	AFM	FM	AFM
Cr-imp	4.388	-3.690	4.334	-3.802	4.248	-4.058	4.335	-3.988
Cr-1st	3.602	3.364	3.704	3.425	3.543	3.343	3.735	3.485
In(Cd)-1st			0.043	-0.067	0.044	-0.108	0.063	-0.104
As [CrAs]-3rd	-0.405	-0.405	-0.412	-0.413	-0.418	-0.418	-0.025	-0.074
As(Se) [Inter]-3rd			-0.202	-0.237	-0.305	-0.352	-0.105(Se)	-0.110(Se)
As(Se) [SC]-3rd			-0.025	-0.067	-0.032(Se)	-0.059(Se)	-0.417(Se)	-0.418(Se)
Cr at Void2 site	BULK CrAs		CrAs/InAs		CrAs/CdSe-1		CrAs/CdSe-2	
	FM	AFM	FM	AFM	FM	AFM	FM	AFM
Cr-imp	3.901	-2.908	3.821	-3.262	3.729	-3.263	4.171	-3.551
Cr-1st	3.419	3.267	3.412	3.225	3.300	3.103	3.467	3.335
In(Cd)-1st			0.014	-0.176	-0.118	-0.030	0.023	-0.038
As [CrAs]-2nd	-0.341	-0.285	-0.364	-0.323	-0.371	-0.330	-0.470	-0.371
As(Se) [Inter]-2nd			-0.167	-0.141	-0.308	-0.214	-0.102(Se)	-0.104(Se)
As(Se) [SC]-2nd			-0.009	-0.039	-0.013(Se)	-0.033(Se)	-0.033(Se)	-0.026(Se)

the fact that the bulk CrSe presents a larger gap than the bulk CrAs due to the larger electronegativity of the Se atom as it was shown in reference [13]. As a consequence the states of the As atoms at the first interface have moved closer to the Fermi level in a rigid way with respect to the As atoms in the CrAs layer. Cd atoms at both interfaces show similar DOS to the In atoms in the CrAs/InAs interface. Se atoms within the CdSe layer show a similar shape to the As atoms in the InAs layer while Se atoms at the second interface show states deeper in energy than the As atom in the first interface in agreement with the larger gap-width shown by the Cr atoms in the second interface with respect to the first CrAs/CdSe interface.

3. Cr impurities

We will start our discussion from the case of Cr impurities. The first case under study is when Cr impurity atoms are located at As(Se) or Void2 sites at the interface. With respect to the perfect Cr sites where the first neighbors were four sp atoms and four voids, the Cr impurity atoms have now as nearest neighbors two Cr atoms and two In(Cd) atoms

together with two Void1 and two Void3 sites. Thus the local environment of the Cr impurities is fundamentally different. In the case of Cr impurities at As and Void2 sites in the bulk, we have shown that the spin magnetic moment could be either ferromagnetically (FM) coupled to the spin moment of the Cr atoms at the perfect sites or antiferromagnetically (AFM) coupled with the latter one being the energetically favorable case [26]. The AFM was occurring due to the short distance between the Cr impurity atoms and its four nearest Cr neighbors (Cr as well as Mn atoms are known to have antiparallel spin moments under a critical distance). In the case of the interfaces under study the Cr impurity atoms have now two instead of four nearest Cr neighbors as in the bulk. But it seems that this is enough to have again two stable solutions, a FM and an AFM one, depending on the starting potential, for both Cr at interfacial As(Se) and Void2 sites. The AFM solution seems energetically more favorable although we have not converged the energetics of the defects (for the reason see discussion in reference [26]).

In figure 3 we have gathered the atom-resolved DOS for the Cr impurity atoms and its nearest Cr neighbors for all three interfaces under study and

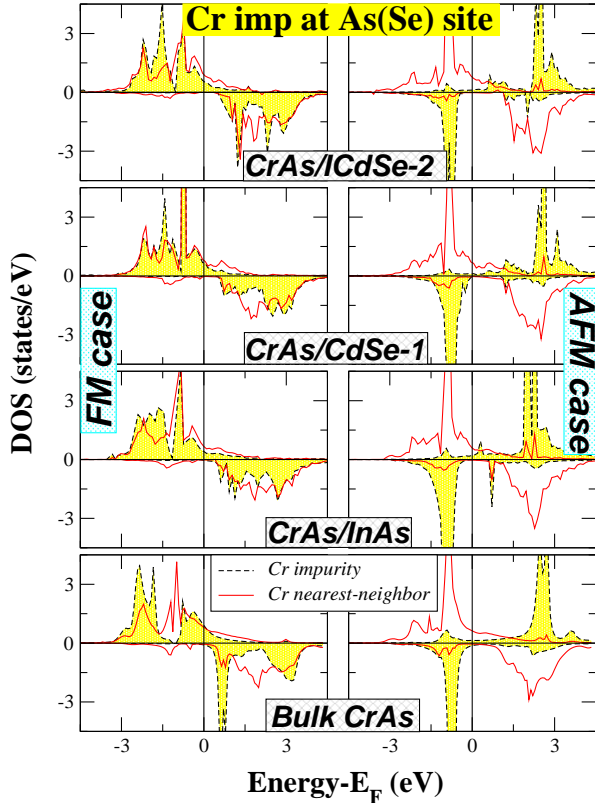


Fig. 3. (Color online) Cr-resolved DOS for the case of Cr impurity atoms at interfacial As(Se) sites at in the case of the ferromagnetic (FM) [left panel] and antiferromagnetic coupling (AFM) [right panel] between the Cr impurity atom and its Cr nearest-neighbors (see text for details). Details as in figure 2.

bulk CrAs for the case of Cr impurity at As(Se) site and for both the FM and AFM cases. Results are similar when the Cr impurity is located at the Void2 site and thus are not shown here. Also results are in all cases similar to the bulk one with minor changes at the position of the peaks due to the variation in the environment surrounding the impurities. In the FM case the impurities show almost zero occupied minority-spin states while the Cr nearest neighbors show a very small weight of minority-spin states below the Fermi level. In all cases the half-metallic character of the interface is not affected. In the AFM case the Cr impurities exhibit a large spin-splitting of the bands and almost all the spin-down states are occupied while almost all spin-up states are empty. This leads to a large gap in the spin-down band between the spin-down occupied bands of the impurity atom and the unoccupied spin-down bands of the Cr nearest neighbors and the half-metallic character of the interface is not affected. In table 2 we have gath-

Table 3

Atom-resolved spin magnetic moments in μ_B for the case of Cr impurity atoms at interfacial Void1, In(Cd) and Void3 sites in the case of the three interfaces under study. Notation as in table 2.

Cr at Void1 site	CrAs/InAs	CrAs/CdSe-1	CrAs/CdSe-2
Cr-imp	3.522	3.363	3.686
As(Se) [CrAs]-1st	-0.300	-0.299	-0.296
As(Se) [Inter]-1st	-0.151	-0.275	-0.042
Cr [Inter]-2nd	3.448	3.352	3.622
Cr at In(Cd) site	CrAs/InAs	CrAs/CdSe-1	CrAs/CdSe-2
Cr-imp	3.185	3.311	4.015
As(Se) [SC]-1st	-0.157	-0.095	-0.147
As(Se) ([Inter]-1st	-0.324	-0.406	-0.254
Cr [Inter]-3rd	3.328	3.252	4.219
Cr at Void3 site	CrAs/InAs	CrAs/CdSe-1	CrAs/CdSe-2
Cr-imp	3.508	3.501	3.833
As(Se) [SC]-1st	-0.024	-0.004	0.009
As(Se) [Inter]-1st	-0.135	-0.275	-0.025
Cr [Inter]-2nd	3.478	3.384	3.635

ered the atomic spin magnetic moments for all cases mentioned above. We can see that spin moments behave similar to the case of the Cr impurities at As or Void2 sites in the perfect bulk. In the FM case the Cr impurity atoms have a larger spin moment with respect to the Cr atoms in the perfect systems since the weight of the minority occupied states has vanished as a result of the hybridization with its first neighbors. The Cr atoms which are first neighbors of the impurity atoms present spin moments almost identical to the perfect compounds in table 1. In the AFM case although it seems from the DOS that all five spin-down d -states of the impurity atom are occupied the spin moment is less than $5 \mu_B$ since some spin-up states also appear below the Fermi level reflecting the band-structure of the Cr nearest neighbors. We should note that spin moments are slightly smaller when the impurity is located at a Void2 instead of a As(Se) site because although the nearest-neighbors are the same, the next-nearest and further neighbors are different. We should finally note here that the AFM case is the most interesting case for applications since the occurrence of half-metallic ferrimagnetism leads to smaller external fields and exhibiting smaller energy losses with respect to ferromagnets.

The next case under study is when the Cr impurity is located at a Void1 site. Although the Void1

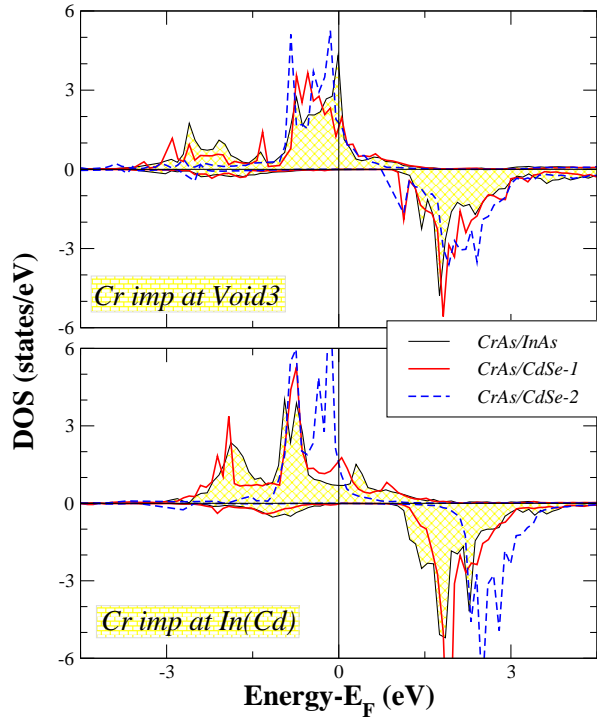


Fig. 4. (Color online) Density of states of the Cr impurity atom at Void3 (upper panel) and In(Cd) (lower panel) interfacial sites for all the interfaces under study. Details as in figure 2.

site is located in the same layer as the Cr atoms, they are second neighbors having the same nearest neighbors (four sp atoms and four voids). Thus we do not expect Cr impurities at Void1 sites to alter the electronic and magnetic properties of the interface similarly to the situation of Cr impurities at Void1 sites in the bulk CrAs [26]. The DOS is similar to the Cr atoms in the perfect systems and thus we do not present them since the gap is almost unaltered and the half-metallicity is not affected. The spin magnetic moment of the Cr impurity atoms which are shown in table 3 are slightly larger than the Cr atoms in the perfect system by about $0.2 \mu_B$. The Cr nearest-neighbors have spin moment almost identical to the Cr impurities and thus part of the charge of the Cr impurity atoms is used to increase the spin moment of the Cr second neighbors with respect to the perfect interfaces.

The final case under study in this section is when the Cr impurity occurs at the In(Cd) sites at the interface or the Void3 sites which are located in the same layer with the In(Cd) ones. Although one could think that these impurities should destroy the half-metallic character of the interface, this is not true.

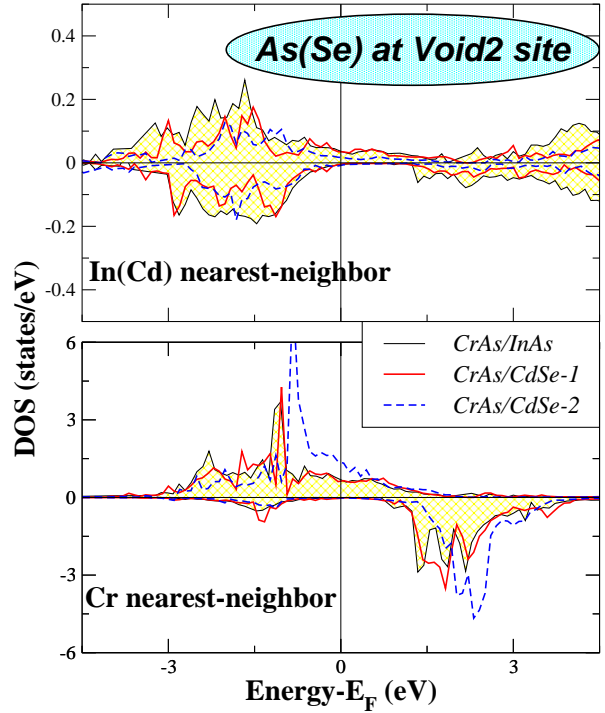


Fig. 5. (Color online) In the case of As(Se) impurities at Void2 sites we present the atom-resolved DOS of the nearest Cr and In(Cd) neighbors for all three interfaces. Details as in figure 2.

Cr impurities at these sites have as nearest neighbors two As(Se) atoms in the semiconducting space and two As(Se) site at the interface. Thus their local environment is quite close to the one of the Cr atoms at the perfect interface sites. As a result the half-metallic character is not destroyed as shown by the DOS in figure 4. When the impurity is located at a Void3 site, there is almost no-occupied spin-down states while when the impurity is located at the In(Cd) site the weight of the occupied spin-down states is very small and the width of the gap is comparable to the perfect compounds in figure 2. In the latter case we see that for the CrAs/CdSe-2 interface the bands are slightly shifted to higher energy as in a rigid-band model with respect to the other interfaces but the gap has even larger width. This is reflected also to the spin-magnetic moments presented in table 3 where for this case the Cr impurity spin moment exceeds the $4 \mu_B$ while for the other interfaces it is slightly larger than the perfect systems.

4. As(Se) impurities

Next we will present our results on the As impurities in the case of the CrAs/InAs and CrAs/CdSe-1 interfaces and on the Se impurities in the case of the CrAs/CdSe-2 interface. We have studied all possible cases and in table 4 we have concentrated the atom-resolved spin magnetic moments for the impurities and their nearest neighbors. The DOS of the impurities in general present no large variation with respect to the As(Se) atom at the interface or the case of impurities at the perfect bulk and thus we present only the case of As(Se) atom at Void2 sites, where the As(Se) impurity atom has the same nearest-neighbors as at the perfect interfacial As(Se) sites. In all other cases the impurity atom has four As(Se) atoms as nearest neighbors (two at the interface and two at the CrAs, when the impurity is located at the Cr or Void1 sites, and two at the InAs(CdSe) layer, when it is located at the In(Cd) or Void3 sites).

We will first discuss the case of As(Se) impurities at the Cr and Void1 sites. At the same energy window with the d electrons of the Cr atoms are located the p electrons of the As(Se) atoms. The DOS of the impurity atoms is similar to the case of As(Se) impurities at Cr and Void1 sites in bulk CrAs(CrSe) presented in [26] and thus we do not present them. For the interfacial As(Se) atoms in the perfect interfaces the minority p states of As(Se) are completely occupied leading to small negative spin moments (see table 1). The impurity As(Se) atoms at Cr or Void1 sites, on the other hand, have four other As(Se) atoms as nearest neighbors and thus the p states of the As(Se) impurity atoms have to hybridize with the p states of the neighboring As(Se) atoms which are almost completely occupied instead of the Cr t_{2g} states for which only the majority states are occupied leading to occupancy of the antibonding p spin-up states and to positive spin magnetic moments as shown in table 4. Due to the reorganization of the charge induced by the impurity As(Se) states, the number of the occupied spin-up p -states of the neighboring As(Se) atoms increases and, although the spin magnetic moments remain negative, their absolute value decreases. In all cases discussed just above, the impurity states are not located in the gap similar to the what happened for the same impurities in the bulk systems (see [26]) and the half-metallicity is preserved.

When the As(Se) atoms migrate to Void2 sites, their nearest neighbors remain two Cr and two

Table 4

Atom-resolved spin magnetic moments in μ_B for the case of As(Se) impurity atoms at various interfacial sites in the case of the three interfaces under study. Notation as in table 2.

As(Se) at Cr site	CrAs/InAs	CrAs/CdSe-1	CrAs/CdSe-2
As(Se)-imp	0.108	0.118	0.127
As(Se) [CrAs]-1st	-0.243	-0.255	-0.271
As(Se) [Inter]-1st	-0.061	-0.177	-0.093
As(Se) at Void1 site	CrAs/InAs	CrAs/CdSe-1	CrAs/CdSe-2
As(Se)-imp	0.143	0.084	0.070
As(Se) [CrAs]-1st	-0.222	-0.267	-0.123
As(Se) [Inter]-1st	-0.114	-0.208	-0.087
As(Se) at Void2 site	CrAs/InAs	CrAs/CdSe-1	CrAs/CdSe-2
As(Se)-imp	0.269	0.207	-0.046
Cr-1st	3.361	3.212	3.367
In(Cd)-1st	0.012	-0.007	-0.010
As(Se) [CrAs]-2nd	-0.318	-0.314	-0.494
As(Se) [Inter]-2nd	-0.104	-0.229	-0.114
As(Se) [SC]-2nd	0.056	0.050	-0.074
As(Se) at In(Cd) site	CrAs/InAs	CrAs/CdSe-1	CrAs/CdSe-2
As(Se)-imp	0.038	0.269	0.048
As(Se) [Inter]-1st	-0.128	-0.013	-0.584
As(Se) [SC]-1st	-0.008	0.287	-0.249
As(Se) at Void3 site	CrAs/InAs	CrAs/CdSe-1	CrAs/CdSe-2
As(Se)-imp	0.093	0.068	0.197
As(Se) [Inter]-1st	-0.069	-0.142	-0.003
As(Se) [SC]-1st	-0.009	-0.013	-0.008

In(Cd) atoms as for the perfect As(Se), but the further neighbors change and the interfacial As atoms are now next-nearest neighbors and the hybridization between their p states is intense leading to occupation of the antibonding spin-up p states and positive values of the spin magnetic moments of the impurity atoms as shown in table 4 for the case of the As impurities in CrAs/InAs and CrAs/CdSe-1 interfaces or to a large variation of the negative Se spin moment in the case the CrAs/CdSe-2 interface (the spin moment of the impurity is half with respect to the Se atom at the perfect sites). The Cr atoms at the interface have now 5 instead of 4 As(Se) atoms as nearest neighbors but the hybridization of the t_{2g} d -states is little affected and the nearest-neighboring Cr spin moments are almost identical to the perfect interfaces. A similar behavior is exhibited by the spin moments of the As(Se) second

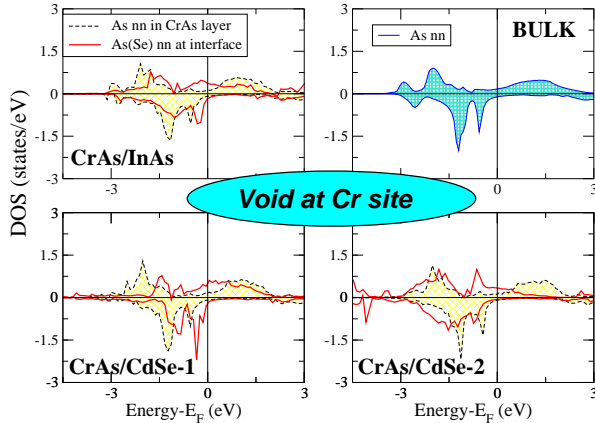


Fig. 6. ((Color online) In the case of Void impurity at an interfacial Cr site we present the atom-resolved DOS of the nearest As(Se) neighbors in the CrAs layer and at the interface for all three interfaces and for the bulk CrAs. Details as in figure 2.

neighbors. The behavior of the spin moments is reflected also in the DOS presented in figure 5. The DOS of the Cr nearest neighbors presents for all interfaces under study a very wide minority-spin gap similar to the perfect compounds with a large spin-splitting between the occupied majority- and the unoccupied minority-spin bands. The shape of the Cr DOS is similar to the Cr atoms at the perfect interfaces shown in figure 2 revealing the small influence of the hybridization with the impurity As(Se) p -states. The same is also valid for the DOS of the nearest In(Cd) atoms shown also in the same figure although the gap is smaller for these atoms similarly to what occurred in the perfect interfaces.

The case of As(Se) impurities at In(Cd) and Void3 sites is more difficult to be understood and although the half-metallicity is preserved the spin moments of the As(Se) impurity atoms and their nearest As(Se) atoms show large variations. In the case of the CrAs/InAs interface the As impurity atom has 4 As atoms as nearest neighbors, in the case of the CrAs/CdSe-1 atom the As impurity atom has two As at the interface and two Se atoms within the CdSe layer as nearest neighbors while in the case of the CrAs/CdSe-2 interface the Se impurity atom has four Se atoms as nearest neighbors. Se atoms have one electron more than the As ones and thus in general a larger number of spin-up states is occupied as revealed also from the spin magnetic moments in table 1. Thus especially when the impurity is located at the In(Cd) site no trend can be found in table 4 regarding the spin magnetic

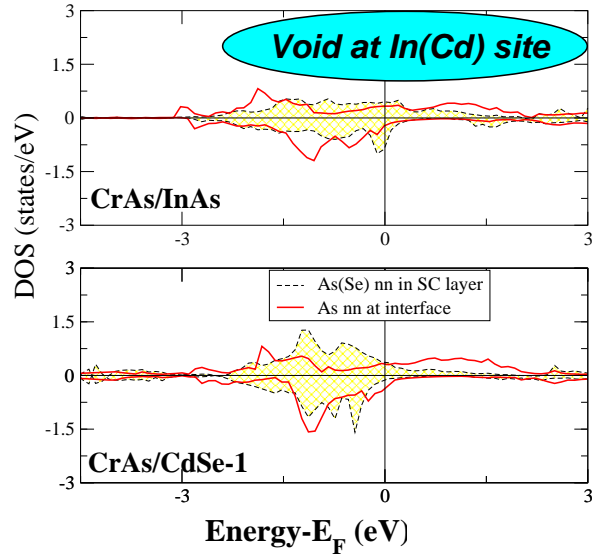


Fig. 7. (Color online) In the case of Void impurity at an interfacial In(Cd) site we present the atom-resolved DOS of the nearest As(Se) neighbors in the semiconducting layer and at the interface for two of the studied interfaces. Details as in figure 2.

moments and the situation is interface-dependent.

5. Void impurities

Up to now we have studied the case of the Cr and As(Se) impurities and in all cases the half-metallicity was preserved. In this section we will study the effect of Voids. Voids are Schottky-type defects with large formation energies. A Void impurity in reality means that an atom is missing leading to a reorganization of the charge of the neighboring atoms. We will start our discussion from the case of a Void at a Cr site and in figure 6 we present the DOS of the nearest As(Se) neighbors for all three interfaces and for the bulk CrAs. In the case of the bulk the missing Cr atom means that As atoms have now three instead of four Cr nearest neighbors and the p -bands of As move closer to the Fermi level without crossing it. In the case of interfaces we should distinguish between the As atoms within the CrAs layer which show a behavior identical to the bulk case and the As(Se) atoms at the interface layer. The latter ones in the perfect multilayers have two Cr atoms and two In(Cd) as nearest neighbors and when a Void occurs at a Cr site they lose one of the two Cr neighbors resulting to a large shift of the p -bands which almost cross the Fermi level. Although one could argue that half-metallicity is present, a

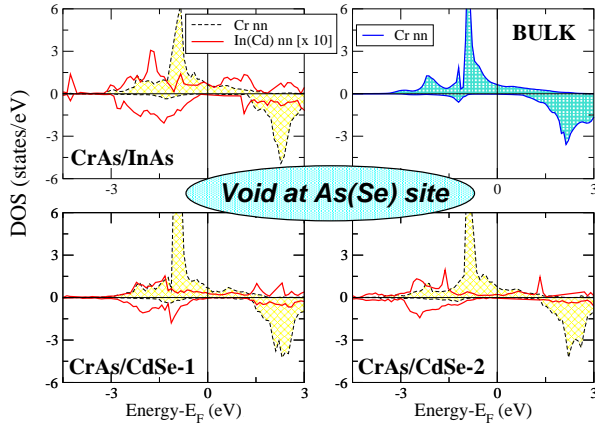


Fig. 8. (Color online) In the case of Void impurity at an interfacial As(Se) site we present the atom-resolved DOS of the nearest Cr and In(Cd) neighbors in the CrAs layer for all three interfaces and for the bulk CrAs. Note that the In(Cd) DOS has been multiplied by a factor of 10. Details as in figure 2.

small change of the lattice constant would lead to loss of the half-metallic character of the perfect interfaces. As the bands move closer to the Fermi level the weight of the spin-up states decreases while the bonding spin-down states are completely occupied leading to larger absolute values of the negative spin moments of the nearest As(Se) neighbors with respect to the perfect case as shown in table 5.

The same phenomenon occurs also when the Void is located at an In(Cd) site as shown in figure 7. The missing In(Cd) neighbors lead to a shift of the p -bands of the nearest-neighbor As(Se) atoms towards higher energies and now clearly the spin-down band crosses the Fermi level destroying the half-metallicity. Especially in the case of the CrAs/InAs interface a spin-down pick is pinned exactly at the Fermi level. In the case of the CrAs/CdSe-1 interface the bands are more narrow; the spin-down pick is located below the Fermi level but a small contraction of the lattice constant could lead to the pinning of the Fermi level at this pick. As discussed for the case of Void impurities at Cr sites, also here the absolute values of the negative spin moments of the neighboring As(Se) atoms increase (see table 5).

The last possible case which can occur is when the Void is located at the interface As(Se) site. The loss of the As(Se) atom only marginally affects the DOS of the Cr atoms at the interface which now have three instead of four neighboring atoms. As shown in figure 8 Cr nearest-neighbors at the interface show similar behavior as in the bulk and the weight of the

Table 5

Atom-resolved spin magnetic moments in μ_B for the case of Void impurities at interfacial Cr, As(Se) and In(Cd) sites in the case of the three interfaces under study. Notation as in table 2.

Void at Cr site	CrAs/InAs	CrAs/CdSe-1	CrAs/CdSe-2
Void-imp	-0.097	-0.129	-0.061
As [CrAs]-1st	-0.592	-0.606	-0.613
As(Se) [Inter]-1st	-0.350	-0.644	-0.159
Void at Ae(Se) site	CrAs/InAs	CrAs/CdSe-1	CrAs/CdSe-2
Void-imp	0.201	0.154	0.190
Cr-1st	3.748	3.691	3.812
In(Cd)-1st	0.033	-0.008	0.017
Void at In(Cd) site	CrAs/InAs	CrAs/CdSe-1	CrAs/CdSe-2
Void-imp	-0.094	-0.073	0.066
As(Se) [Inter]-1st	-0.468	-0.535	-0.210
As(Se) [SC]-1st	-0.141	-0.115	-0.127

occupied minority-spin states is vanishing and the half-metallicity remains robust. The In(Cd) nearest-neighbors exhibit also a large gap as shown in the same figure where the DOS of the In(Cd) has been multiplied by 10 to be visible with respect to the Cr nearest neighbors. The loss of its As(Se) neighbor leads to an increase of the local charge of the Cr nearest-neighbors (in a way they regain the charge which was participating at the bonds with the missing As(Se) atom). This extra local charge occupies spin-up states leading to an increase of the Cr spin moment with respect to the perfect interfaces by about $0.4\text{-}0.5 \mu_B$.

6. In(Cd) impurities

Finally, in the last section we will present our results concerning the case of In, for the CrAs/InAs interface, and Cd, for both CrAs/CdSe interfaces, impurities at various sites. All three interfaces show similar behavior and thus in figure 9 we present the DOS for all possible In impurities for the CrAs/InAs multilayer. We should note that with respect to the conservation of the half-metallicity this is the most interesting case since for the other two CrAs/CdSe interfaces the half-metallic character is conserved for all cases under study. In table 6 we have gathered the atom-resolved spin moments for all cases under study and as it can be easily deduced from the table the variation of the spin moments for the same position of the In(Cd) impurity is similar for all three

Table 6

Atom-resolved spin magnetic moments in μ_B for the case of In(Cd) impurities at various interfacial sites in the case of the three interfaces under study. Notation as in table 2.

In(Cd) at Cr site	CrAs/InAs	CrAs/CdSe-1	CrAs/CdSe-2
In(Cd)-imp	0.001	-0.070	-0.025
As(Se) [CrAs]-1st	-0.357	-0.459	-0.434
As(Se) [Inter]-1st	-0.146	-0.376	-0.074
Cr [CrAs]-3rd	3.299	3.456	3.173
Cr [Inter]-3rd	3.321	3.176	3.464
In(Cd) [Inter]-3rd	-0.014	-0.048	-0.006
In(Cd) at Void1 site	CrAs/InAs	CrAs/CdSe-1	CrAs/CdSe-2
In(Cd)-imp	0.068	0.004	0.033
As(Se) [CrAs]-1st	-0.238	-0.318	-0.283
As(Se) [Inter]-1st	-0.130	-0.269	-0.059
Cr [CrAs]-2nd	3.429	3.571	3.590
Cr [Inter]-2nd	3.427	3.272	3.262
In(Cd) [Inter]-2nd	-0.002	-0.032	0.004
In(Cd) at As(Se) site	CrAs/InAs	CrAs/CdSe-1	CrAs/CdSe-2
In(Cd)-imp	0.100	0.148	0.188
Cr-1st	3.590	3.590	3.746
In(Cd)-1st	-0.024	-0.001	0.019
As(Se) [CrAs]-3rd -0.414	-0.421	-0.416	
As(Se) [Inter]-3rd	-0.209	-0.384	-0.096
As(Se) [SC]-3rd	-0.040	-0.032	-0.023
In(Cd) at Void2 site	CrAs/InAs	CrAs/CdSe-1	CrAs/CdSe-2
In(Cd)-imp	-0.041	0.088	0.063
Cr-1st	3.185	3.256	3.446
In(Cd)-1st	-0.006	-0.020	-0.007
As(Se) [CrAs]-2nd	-0.398	-0.362	-0.475
As(Se) [Inter]-2nd	-0.176	-0.288	-0.102
As(Se) [SC]-2nd	-0.044	-0.039	-0.067
In(Cd) at Void3 site	CrAs/InAs	CrAs/CdSe-1	CrAs/CdSe-2
In(Cd)-imp	0.058	-0.008	0.045
As(Se) [Inter]-1st	-0.073	-0.230	-0.016
As(Se) [SC]-1st	-0.011	-0.028	-0.011
Cr [Inter]-2nd	3.473	3.286	3.638
In(Cd) [Inter]-2nd	0.001	-0.031	0.004
In(Cd) [SC]-2nd	-0.003	0.002	-0.038

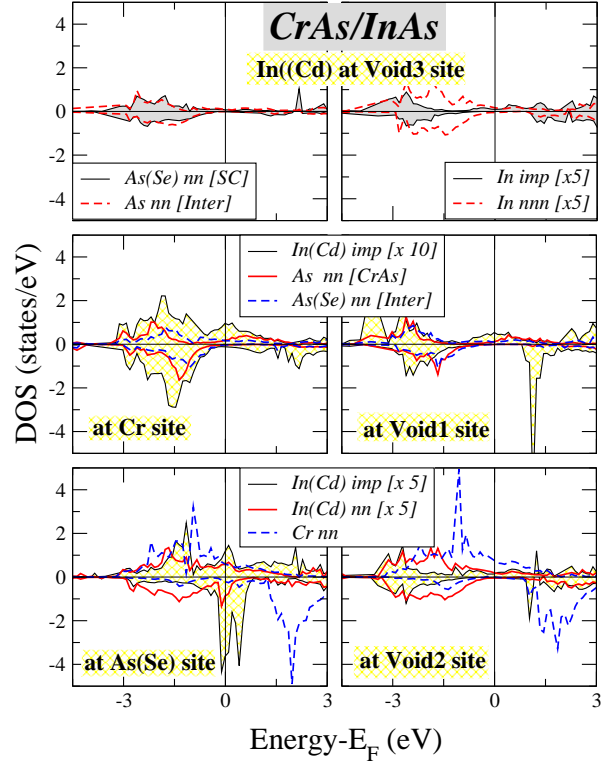


Fig. 9. (Color online) In the case of In(Cd) impurities at various interfacial sites, we present the atom-resolved DOS of the impurity atom and its neighbors. Note that the In(Cd) DOS has been multiplied by a factor of 5 or 10 in all cases. Details as in figure 2.

interfaces and thus we will restrict our discussion to the CrAs/InAs case.

We expect that the most frequent case to occur would be the In impurity at the Cr site since such an impurity does not disrupt the zinc-blende structure. In atoms have only two valence electrons occupying the deep-energy-lying s -states and thus for the energy window which we examine the p -states, which we observe, have their origin at the nearest As neighbors whose p -states penetrate in the In sites (Cd has only one valence s -electron). Thus the In impurity acts similarly to a Void, although it does not lead to such large reorganization of the charge of the neighboring atoms, leading to slightly larger spin moment of the neighboring atoms with respect to the perfect interfaces as shown in table 6. Due to the small weight of the In p -states we have multiplied the corresponding DOS with a factor 5 or 10 in figure 9 to make it visible. With respect to the case of Void impurity at the Cr site, here the shift of the bands of the nearest-neighboring As atoms is smaller keeping the half-metallic character of the in-

interface although the gap is considerably shrinking.

When the In impurity is located at the Void1 site, the disturbance of the lattice is smaller with respect to the case just presented, although both Cr and Void1 sites have the same nearest-neighbors and as shown in figure 9 the width of the gap remains unchanged. Due to the negligible weight of the In p states also the occurrence of In impurities at Void2 and Void3 sites leads to a slight variation of the spin moments but the half-metallicity is preserved and the gap retains a large width. To conclude we should discuss also the case of In impurities at As sites. As atoms at the interface have two Cr atoms as nearest neighbors and the hybridization between the As p - and Cr t_{2g} -orbitals is strong. The substitution of an As atom by an In one leads to reduced hybridization for the Cr orbitals and Cr atoms at the interface regain the charge participating at the bonds with the missing As atom. This extra charge is accommodated at the Cr spin-up states leading to larger spin magnetic moments of the Cr atoms at the interface which now are about $3.59 \mu_B$ instead of $3.25 \mu_B$ in the case of the perfect CrAs/InAs interface presented in table 1. The In impurity atom and its nearest-neighboring In atoms have states within the gap, as shown in figure 9 but if we take into account that we have multiplied the In DOS by 10 their real weight at the Fermi level is negligible with respect to the Cr majority-spin DOS. Thus we can safely consider that the half-metallicity is conserved although as shown by the Cr DOS, the gap in the minority-spin band seriously shrinks and the Fermi level is near the right edge of the gap.

7. Conclusion

We have studied using the Korringa-Kohn-Rostoker method the appearance of single impurities at interfaces between the half-metallic ferromagnet CrAs and the binary InAs and CdSe semiconductors. In the case of bulk CrAs studied in reference [26] we had shown that most impurities affect the half-metallic character of CrAs inducing states either at the edges of the gap or in the middle of the gap. But multilayers are very thin as experiments show [9] and thus we cannot use the impurity calculations for the bulk to discuss the case of interfaces. We have studied all possible single impurities at the interfaces. Contrary to the bulk systems almost all defects were not affecting the half-metallic character of the perfect interfaces.

The only exception were Void impurities at Cr or In(Cd) sites. The missing Cr or In(Cd) atom leads to a reorganization of the charge of the surrounding atoms and as a result the p bands of the nearest neighboring As(Se) atom shift to higher energies crossing the Fermi level and leading to loss of the half-metallicity. This is the opposite behavior that the one exhibited by the Void impurities at Cr site in the bulk CrAs alloy where the DOS remained almost unchanged [26]. The different behavior of the Void impurities should be attributed to the lower dimensionality of the interfaces with respect to the bulk. But Void impurities are Schottky-type and we expect them to exhibit high formation energies and thus their number should be small in the experimental systems. Thus contrary to the bulk CrAs and eventually thick films showing a bulk-like behavior, impurities are expected to affect only marginally the half-metallic character of the interfaces in the case of thin multilayers and the latter ones are promising for spintronic devices.

References

- [1] M.N. Baibich, J.M. Broto, A. Fert, F. Nguyen Van Dau, F. Petroff, P. Etienne, G. Creuzet, A. Friederich, J. Chazelas, Phys. Rev. Lett. 61 (1988) 2472.
- [2] G. Binasch, P. Grünberg, F. Saurenbach, W. Zinn, Phys. Rev. B 39 (1989) 4828.
- [3] I. Žutić, J. Fabian, S. Das Sarma, Rev. Mod. Phys. 76 (2004) 323.
- [4] H. Zabel, Materials Today 9 (2006) 42; H. Zabel, Superlattices and microstructures 46 (2009) 541.
- [5] S.P. Dash, S. Sharma, R.S. Patell, M.P. de Jong, R. Jansen, Nature 462 (2009) 491.
- [6] M.I. Katsnelson, V. Yu. Irkhin, L. Chioncel, A. I. Lichtenstein, R. A. de Groot. Rev. Mod. Phys. 80 (2008) 315.
- [7] R.A. de Groot. F.M. Mueller, P.G. van Engen, K.H.J. Buschow, Phys. Rev. Lett. 50 (1983) 2024.
- [8] H. Akinaga, T. Manago, M. Shirai, Jpn. J. Appl. Phys. 39 (2000) L1118.
- [9] M. Mizuguchi, H. Akinaga, T. Manago, K. Ono, M. Oshima, M. Shirai, M. Yuri, H.J. Lin, H.H. Hsieh, C.T. Chen, J. Appl. Phys. 91 (2002) 7917.
- [10] K. Ono, J. Okabayashi, M. Mizuguchi, M. Oshima, A. Fujimori, H. Akinaga, J. Appl. Phys. 91 (2002) 8088.
- [11] J.H. Zhao, F. Matsukura, K. Takamura, E. Abe, D. Chiba, H. Ohno, Appl. Phys. Lett. 79 (2001) 2776.
- [12] S. Li Z. Tian, J. Fang, J.-G. Duh, K.-X. Liu, Z. Huang, Y. Huang, Y. Du, Sol. St. Commun. 149 (2009) 196.
- [13] I. Galanakis and Ph. Mavropoulos, Phys. Rev. B 67 (2003) 104417.
- [14] I. Galanakis, Phys. Rev. B 66 (2002) 012406.

- [15] Y.J. Zhao and A. Zunger, Phys. Rev. B 71 (2005) 132403; M.S. Miao and W.R.L. Lambrecht, Phys. Rev. B 72 (2005) 064409; L.J. Shi B.G. Liu, J. Phys.: Condens. Matter 17 (2005) 1209; B. G. Liu, Phys. Rev. B 67 (2003) 172411.
- [16] M. Shirai, J. Phys.: Condens. Matter 16 (2004) S5525; M. Shirai, M. Seike, K. Sato, H. Katayama-Yoshida, J. Magn. Magn. Mater. 272-276 (2004) 344.
- [17] K. Nakamura, Y. Kato, T. Akiyama, T. Ito, A.J. Freeman, Phys. Rev. Lett. 96 (2006) 047206.
- [18] W.H. Xie, Y.-Q. Xu, B.-G. Liu, D.G. Pettifor, Phys. Rev. Lett. 91 (2003) 037204.
- [19] L. Chioncel, Ph. Mavropoulos, M. Ležaić, S. Blügel, E. Arrigoni, M.I. Katsnelson, A.I. Lichtenstein, Phys. Rev. Lett. 96 (2006) 197203.
- [20] Ph. Mavropoulos, I. Galanakis, P.H. Dederichs, J. Phys.: Condens. Matter 16 (2004) 4261.
- [21] C.Y. Fong, M.C. Qian, J.E. Pask, L.H. Yang, S. Dag, Appl. Phys. Lett. 84 (2004) 239; M. Moradi and Z. Soltani, J. Appl. Phys. 105 (2009) 023701; F. Ahmadian, M.R. Abolhassani, M. Ghoranneviss, M. Elahi, Physica B: Condens. Matter 404 (2009) 3684.
- [22] E. Şaşıoğlu, I. Galanakis, L.M. Sandratskii, P. Bruno, J. Phys.: Condens. Matter 17 (2005) 3915.
- [23] I. Galanakis, K. Özdoğan, E. Şaşıoğlu, B. Aktaş, Phys. Rev. B 74 (2006) 140408(R); K. Özdoğan, I. Galanakis, B. Aktaş, E. Şaşıoğlu, J. Magn. Magn. Mater. 320 (2008) 197.
- [24] M. Ležaić, Ph. Mavropoulos, J. Enkovaara, G. Bihlmayer, S. Blügel, Phys. Rev. Lett. 97 (2006) 026404; L. Chioncel, M.I. Katsnelson, G.A. de Wijs, R.A. de Groot, A.I. Lichtenstein, Phys. Rev. B 71 (2005) 085111; R. Skomski and P. A. Dowben, Europhys. Lett. 58 (2002) 544.
- [25] Ph. Mavropoulos and I. Galanakis, J. Phys.: Cond. Matter 19 (2007) 315221.
- [26] I. Galanakis and S.G. Pouliaxis, J. Magn. Magn. Mat. 321 (2009) 1084.
- [27] N. Papanikolaou, R. Zeller, and P. H. Dederichs, J. Phys.: Condens. Matter 14, 2799 (2002).
- [28] T. Korhonen, A. Settels, N. Papanikolaou, R. Zeller, P.H. Dederichs, Phys. Rev. B 62 (2000) 452; N. Papanikolaou, B. Nonas, S. Heinze, R. Zeller, P.H. Dederichs, Phys. Rev. B 62 (2000) 11118.